Biochemistry

 Volume 39, Number 47 November 28, 2000

New Concepts

Is Counterion Delocalization Responsible for Collapse in RNA Folding?†

Venkatesh L. Murthy and George D. Rose*

Department of Biophysics & Biophysical Chemistry, Johns Hopkins University School of Medicine, 725 North Wolfe Street, 701 Wood Basic Sciences, Baltimore, Maryland 21205-2105

Received August 3, 2000; Revised Manuscript Received October 9, 2000

ABSTRACT: Although energetic and phylogenetic methods have been very successful for prediction of nucleic acid secondary structures, arrangement of these secondary structure elements into tertiary structure has remained a difficult problem. Here we explore the packing arrangements of DNA, RNA, and DNA/RNA hybrid molecules in crystals. In the conventional view, the highly charged double helix will be pushed toward isolation by favorable solvation effects; interactions with other like-charged stacks would be strongly disfavored. Contrary to this expectation, we find that most of the cases analyzed (∼80%) exhibit specific, preferential packing between elements of secondary structure, which falls into three categories: (i) interlocking of major grooves of two helices, (ii) side-by-side parallel packing of helices, and (iii) placement of the ribose−phosphate backbone ridge of one helix into the major groove of another. The preponderance of parallel packing motifs is especially surprising. This category is expected to be maximally disfavored by charge repulsion. Instead, it comprises in excess of 50% of all packing interactions in crystals of A-form RNA and has also been observed in crystal structures of large RNA molecules. To explain this puzzle, we introduce a novel model for RNA folding. A simple calculation suggests that the entropy gained by a cloud of condensed cations surrounding the helices more than offsets the Coulombic repulsion of parallel arrangements. We propose that these condensed counterions are responsible for entropy-driven RNA collapse, analogous to the role of the hydrophobic effect in protein folding.

Advances in ab initio (*1*−*3*) and phylogenetic (*4*) methodologies for prediction of RNA structure now allow routine and accurate predictions of RNA secondary structure. However, automated assembly of secondary structure elements into tertiary structures has remained a challenging problem. Analyses of protein secondary structure arrangements such as Crick's prediction of "knobs into holes" packing of α-helices permitted prediction of the structure of the coiled-coil domain of tropomyosin (*5*). Similarly, Richards and co-workers (*6*, *7*) were able to predict the tertiary structure of myoglobin using the "ridges into grooves" observation of Chothia (*8*).

"Groove-fitting" nucleic acid packing motifs have been previously observed (*9*, *10*). These motifs either interlock the major grooves from two double helices or place a ribose−phosphate backbone ridge of one double helix into a groove of another. Crystal structures of RNA molecules containing side-by-side arrangements of double helices have shown a preponderance of parallel packings (*11*−*14*). Neither the generality nor a physical basis for any of these motifs has been established.

Here, we present an analysis of helix packing preferences in crystals of simple RNA, DNA, and hybrid molecules and

† Supported by Johns Hopkins' Medical Scientist Training Program and NIH Grant GM07309 (V.L.M.) and by NIH Grant GM29458 and The Mathers Foundation (G.D.R.).

* Corresponding author. Phone: (410) 614-3970. Fax: (410) 614-3971. E-mail: rose@grserv.med.jhmi.edu.

10.1021/bi001820r CCC: $19.00
Published on Web 11/02/2000

an explanatory entropy-driven model for RNA folding that draws upon Manning's theory of counterion condensation (*15*, *16*).

METHOD

We calculated the crossing angles for nucleic acid duplexes in crystals classified by the NDB (*17*) as containing only simple double-helical B-form DNA, A-form DNA, A-form DNA/RNA hybrids, or A-form RNA. Structures classified by the NDB as containing base triples were excluded. Only structures with exactly one duplex per asymmetric unit and with at least three phosphate groups per strand and six per asymmetric unit were included. Helix axes were determined using the rotational least-squares method (*18*). For structures with overhanging phosphates, helix end points were determined by taking the average of the projections of the two terminal phosphorus atoms onto the helix axis. The majority of structures lacked both 5′ and 3′ overhanging phosphates. For these structures, end points were determined by projecting either the two terminal 5′ phosphorus atoms or the two terminal 3′ phosphorus atoms onto the helix axis and choosing the maximally separated pair, usually the two 3′ phosphorus atoms. Only those crossings where the distance of closest approach between the two helix axes was less than 25 Å were tabulated. This distance is slightly larger than the diameter of nucleic acid duplexes.

Helix crossing angles (ω) were determined as the dihedral angle given by the points defining the segment of closest approach between the two helix axes and the two distal end points of the helix axes. Note that a crossing only occurs when the segment of closest approach lies between the ends of the helix axes or when the helices are parallel and have overlapping projections. Because there are only 180° of unique crossing angles, values greater than +90° or less than −90° were folded over into the region between those two values. The crossings were grouped into 15° bins by crossing angle and into 1 Å bins by distance of closest approach. Walther et al. (*19*) showed that, in the absence of specific preferences, the probability of a given crossing angle between two finite segments is proportional to the square of the sine of that angle due to geometric considerations. Our data are presented both normalized by this factor and in unmodified form.

RESULTS

Crossing angles and separations from 151 B-form DNA structures, 45 A-form DNA structures, 22 A-form DNA/RNA hybrid structures, and 16 A-form RNA structures (Table 1, Supporting Information) were calculated, and the resulting data are summarized in Table 2 (Supporting Information).

A scatter plot of crossing angle vs separation distance shows several clusters (Figures 1 and 2). A large, well-defined cluster of B-form DNA crossings occurs with an average separation of approximately 16 Å and an average crossing angle of approximately −35°. In this arrangement, the major groove of one helix is packed into the major groove of another helix, usually in or near van der Waals contact (Figure 3a). Although A-form DNA and A-form RNA/DNA hybrid molecules also exhibit this crossing pattern, albeit with a slightly higher crossing angle, this motif seems to be less favored for these molecules.

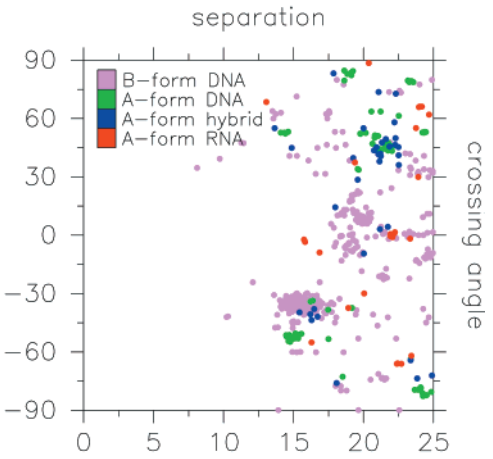

FIGURE 1: Crossing angle and separation data are plotted from B-form DNA (violet), A-form DNA (green), A-form hybrids (blue), and A-form RNA (orange). Several clusters are apparent. Values near −30° and 16 Å correspond to groove into groove packings and place the two duplexes in or near van der Waals contact. Similarly, parallel packings with values near 0° and 20 Å also place the two duplexes in or near van der Waals contact. Finally, a cluster centered near +45° and 22 Å corresponds to ridge into groove packing and is not usually in direct van der Waals contact.

A slightly more dispersed group of B-form DNA crossings has crossing angles near 0° and separations near 20 Å, placing the two helices in an essentially parallel arrangement, again in or near van der Waals contact (Figure 3b). This arrangement is also a favored conformation for A-form DNA/RNA hybrid and A-form RNA molecules, although usually with slightly larger separations between helices.

The third significant cluster has crossing angles near +45° and separations near 22 Å. This motif, which is frequently observed for A-form DNA and A-form DNA hybrid molecules, places the ribose−phosphate backbone "ridge" of one molecule into the major groove of another, often without direct van der Waals contact (Figure 3c). Examination reveals that this packing does not require complete burial of any phosphate groups because of the curved surfaces involved, even when the two molecules are in van der Waals contact.

Crossing frequencies in 15° bins are plotted in both unnormalized form (Figure 2a) and normalized by the expected distribution for purely random crossings (*19*) (Figure 2b). Even without normalization, it is evident that these three motifs (i.e., parallel, groove into groove, and ridge into groove) account for nearly all observed crossings, typically ∼80%. However, different classes of molecules typically favor only one or two of the three categories. The normalized plot, in which the scale represents preferences and antipreferences as energies, clearly shows that only these three motifs have negative energies, reflecting their significant enhancement relative to the random distribution.

DISCUSSION AND THEORY

Nearly every report of the crystal structure of a complex RNA expresses surprise that parallel or nearly parallel arrangements of helices are observed (*11*−*14*). Our analysis of packing interactions in crystal structures of nucleic acids suggests that parallel, side-by-side packing of double helices is actually a highly frequent occurrence. Additionally, nearly all other packing interactions fall into either groove into groove (negative ω) or ridge into groove (positive ω) packing

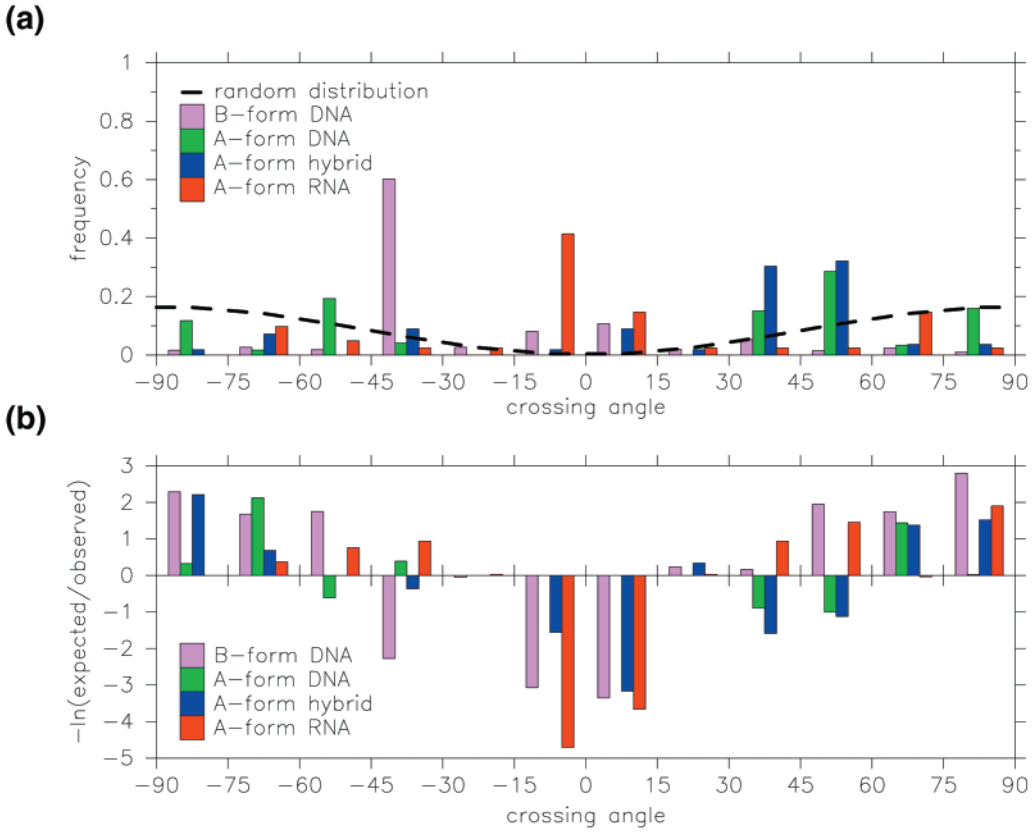

FIGURE 2: (a) The 606, 119, 56, and 41 crossings from B-form DNA (violet), A-form DNA (green), A-form hybrids (blue), and A-form RNA (orange), respectively, are grouped into 15° bins. The resulting populations were then converted into frequencies by dividing by the total number of observed crossings for that category, and they are plotted without further normalization. The dashed line represents the distribution expected in the absence of preferences (*19*). (b) The frequencies are also plotted normalized by the expected random distribution [dashed line in (a)]. The vertical scale in this plot approximates the energetic bias toward or against an individual conformation, in units of kT. For both (a) and (b), each bar within a group of four represents the population within the entire 15° interval.

motifs. These two motifs had been noted previously in the crystal structures of DNA double helices (*9*, *10*). For B-form DNA, where the major groove is large, groove into groove packing predominates. For A-form DNA and A-form DNA/RNA hybrids, both of which have narrower major grooves, ridge into groove packing is preferred over groove into groove packing. Finally, for A-form RNA, which generally has the narrowest major grooves of the four classes of molecules examined, parallel packing arrangements are preferred.

It must be noted, that a number of caveats arise from the fact that our observations are from crystal structures. First, it is possible that the lattice constraints in conjunction with stacking and other interactions bias the distribution of helix crossings. However, the helix axes are aligned with unit cell diagonals in many examples, and in these cases it is possible to retain stacking interactions and lattice integrity regardless of crossing angle. Other potential sources of bias are the presence of crystallization salts such as spermine and spermidine and of crystallization agents such as poly(ethylene glycol). Finally, loops connecting helical elements in complex RNA structures may be the source of substantial bias toward or away from particular interhelical crossing angles. Nonetheless, the magnitude of the biases observed suggests that similar biases will exist in solution, although they might differ in detail.

Counterion Delocalization Effect. In the absence of specific Mg^{2+} binding, it is often believed (*20*) that parallel packing arrangements will be disfavored because they bring many negatively charged phosphate groups into proximity. However, confronted with the preponderance of such packings in crystal structures, often with neither space nor electron density for cations near the interacting surfaces, it appears that this arrangement is actually favorable. Three different models have been invoked to describe attraction between like-charged moieties, including very long DNA molecules: counterion condensation (*21*, *22*), induced dipole effects (*23*), and hydration effects (*24*). All three models can be shown to favor parallel packing. Here, we further explore only the first.

Manning's counterion condensation theory (*15*, *16*) and numerous experiments (reviewed in ref *25*) suggest that a substantial population of cations is "condensed" into a small volume surrounding a charged rod with DNA- or RNA-like linear charge density. These counterions are not bound to any particular site but instead are free to roam about the surface of the nucleic acid; i.e., they are "territorially" bound. They obey neither Langmuir isotherms nor any other laws or equations pertinent to site binding equilibria such as mass action. For example, for the sodium salt of DNA or RNA in water at 298 K, approximately 0.76 sodium ion is associated with the polymer per phosphate, *regardless of the overall sodium concentration*. This proportion remains largely unchanged, regardless of which monovalent species is provided. The corresponding critical number for divalent cations is approximately 0.44 per phosphate.

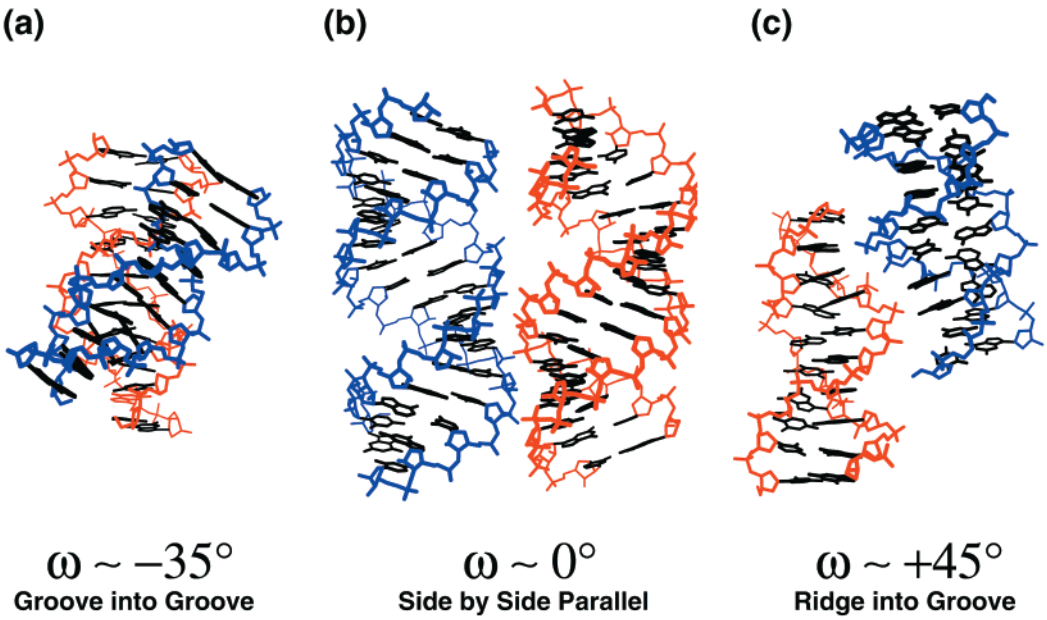

FIGURE 3: Examples of (a) groove into groove, (b) parallel, and (c) ridge into groove packing are illustrated. (a) Groove into groove packings orient the two duplexes with a negative crossing angle and with close separations, interlocking the major groove of one molecule into the major groove of the other. For example, this crossing taken from NDB entry bd0025 (*35*) has a crossing angle of −38.5° and a distance of closest approach between the helix axes of 19.5 Å. This view places both helix axes approximately in the plane of the paper and the line segment defining the closest approach of the two duplexes perpendicular to the plane of the paper. Most examples of this packing motif result in substantial van der Waals contacts. (b) Parallel packings have crossing angles near 0° and also place the two duplexes in or near van der Waals contact. This packing, observed in NDB entry ar0002 (*36*), orients two double helices with a crossing angle of 0.5° and a minimum separation between helix axes of 21.9 Å. (c) Ridge into groove packings place the ribose−phosphate backbone of one helix into the major groove of another. These packings have positive crossing angles and are usually somewhat further spaced than either of the other motifs. A particularly tight example of this type of packing is illustrated from NDB entry bd0025 (*35*). Here, the crossing angle is +38.4°, and the minimum distance between helix axes is only 16.1 Å. In this view, the axis of the red duplex is in the plane of the page and oriented vertically. The axis of the blue duplex is tilted out of the plane of the page so that the top portion of the axis protrudes out of the plane of the paper. This motif is particularly common for A-form DNA and A-form hybrid molecules where, typically, the spacing between helices is near 22 Å, precluding direct van der Waals contacts.

Although Manning's formalism was developed initially for infinitely long electrolytes, several experimental and theoretical studies have upheld its validity for short nucleic acid helices (≤∼12 base pairs) (*26*), *providing that the ratio of cations to phosphates is much greater than unity* (*27*). Under physiological and experimental folding conditions, where this proviso is typically satisfied, the reduction of condensed counterions due to end effects is less than 5% (*26*). We are assuming that this deviation can be safely ignored but with the caveat that end effects require further detailed analysis.

Manning theory treats the electric field about a nucleic acid molecule as being relatively uniform. That is, the field strength at nearly any locale on the surface of the nucleic acid is within kT energy units of nearby locales. Consequently, cations associated with the nucleic acid through outer-sphere complexes will be continually pushed about its surface by thermal motion. The phenomenon of counterion condensation arises from concurrent maximization of the favorable electrostatic interactions between the counterions and the polyelectrolyte and minimization of the entropy loss due to site-specific binding. In contrast, substantial nonuniformities in the electrostatic potential are required to overcome the entropic penalty of confining ions to specific sites.

When two helices are brought together in an essentially parallel orientation, as observed in crystals of short nucleic acid duplexes (Figure 3b), the resulting electric field will be nearly as uniform as for a single isolated helix. Consequently, condensed cations can further delocalize into the larger combined volume surrounding the two helices, resulting in a substantial entropic gain. Applying this idea, we estimate for the attraction between two double helices of length 12 nucleotides (48 nucleotides total) (see Appendix). Although imprecise, the magnitude of attraction can be bounded reliably by selectively overestimating repulsive interactions and underestimating attractive interactions. We obtain a useful lower limit to the magnitude of attraction between helices: $\Delta G_{\text{interaction}} \leq -2.1$ kcal/(mol·pair of helices) in monovalent salts and $\Delta G_{\text{interaction}} \leq -1.5$ kcal/(mol·pair of helices) in divalent salts. Because a number of attractive interactions were entirely omitted and those that were included were underestimated, the actual numbers are likely to be substantially higher.

However, if the two helices are not oriented in an approximately parallel manner, there will be significant minima in the electrostatic potential about the complex. Specifically, for nonparallel packings, ions in locations near the crossing site will be subjected to substantially higher electrostatic field strengths than those in locations far from the crossing site. These extrema will confine counterions, nullifying and perhaps even reversing any entropic gain. This strong orientational dependence of the counterion delocalization effect can explain the distribution of helix crossing angles in crystals of simple nucleic acids and the developing trend seen in structures of more complex RNAs.

Because of the increase in net linear charge density upon formation of a pair of duplexes, it is plausible to assume

that the total number of condensed counterions, which were assumed to be constant in our calculations, will increase slightly. This increase is consistent with the observations that RNAs usually fold more readily in the presence of higher bulk counterion concentrations and that they are more stable in the presence of divalent cations than monovalent cations. A similar linkage model was used to explain the cation dependence of the thermal denaturation of tRNA (*28*).

Another source of counterion concentration dependence in RNA folding and collapse may arise from the observation that the number of condensed counterions is not strictly independent of bulk counterion concentration for relatively short polyelectrolytes (*27*). Although the extent of this deviation can be quite severe at near zero bulk counterion concentrations, over the more relevant concentration range of 1−100 mM for Na^+, the number of condensed cations per phosphate drops from ideality by less than 10% at the low end of the range for helices with 10 or more base pairs (*26*). Consequently, at lower bulk counterion concentrations, the reduction in the number of condensed counterions will result in (1) a proportional reduction in the favorable delocalization entropy and (2) an increase in the net uncompensated charge on the phosphates, thereby increasing the unfavorable Coulombic repulsion between the helices.

In our formulation, the attractive, entropic component of this interaction is directly dependent on the average length of the two duplexes, while the repulsive electrostatic component varies as the square of average length. This competing relationship immediately suggests that there exists some length beyond which two duplexes will not be attracted to each other. It is likely that additional effects, such as electrostatic screening or induced dipole effects, serve to mask this maximum.

Counterion Delocalization Model for RNA Folding. We propose that an entropic attraction mechanism deriving from Manning's theory of counterion condensation (*15*, *16*) best explains recent experiments (*29*, *30*) suggesting a rapid electrostatic collapse in the early stages of RNA folding. Other experiments (*31*, *32*) have shown that increases in entropy drive the docking of the substrate helix into the active site of the *Tetrahymena* ribozyme. Although site-specific binding of Mg^{2+} cations to the RNA backbone may contribute favorably to the energetics of folding (*20*), the contribution from the cloud of condensed counterions appears to be of at least comparable importance, as suggested by recent experiments (*33*). The role of condensed counterion delocalization in driving RNA folding can be compared to the hydrophobic effect in protein folding; both promote structural compaction and are entropy driven. The hydrophobic effect arises from liberation of solvent, namely, water, from the surface of hydrophobic moieties, whereas the counterion delocalization effect is the result of partial liberation of cosolvent, namely, condensed counterions, on the surface of RNA. Just as covalent bond formation between atoms of similar electronegativity is driven by delocalization of valence electrons, not by increased electrostatic interactions, the assembly of RNA helices during collapse and folding is likely to be driven by the delocalization of condensed counterions.

Our model differs from a recent proposal (*20*) which suggests that clusters of site-specifically bound counterions can be viewed as the "hydrophobic" core for RNA folding. That model envisions the assembly of negatively charged helical domains around a positively charged core of Mg^{2+} ions resulting in favorable Coulombic interactions, with no role played by condensed, delocalized cations.

In summary, we propose a *counterion delocalization model* for RNA collapse and folding. This model rationalizes the parallel packing motifs seen in many recently reported crystal structures (*11*−*14*), and it predicts that this motif will be among the dominant motifs seen for complex RNAs.

ACKNOWLEDGMENT

We thank Rajgopal Srinivasan, Rohit Pappu, Teresa Prytzycka, L. Mario Amzel, Vinod Misra, David Draper, Ross Shiman, Jon Lorsch, and Trevor Creamer for useful discussions. We are especially grateful to Bertrand García-Moreno.

APPENDIX

Estimating the Minimum Energy of Attraction between Two Nucleic Acid Helices. For helices of length 12 base pairs, approximately 18 monovalent or 11 divalent counterions are confined to the local neighborhood of each helix; these are the condensed counterions. If two helices are brought together in a parallel manner, the condensed cations can mix together and delocalize into a larger combined volume, resulting in a significant entropic gain (*21*, *22*). Assuming no increase in the quantity of condensed counterions, this gain, roughly, is given by

$$\Delta G_{\text{entropic}} = \Delta G_{\text{expansion}} + \Delta G_{\text{mixing}} = nRT \ln(V_{\text{two helices combined}}/V_{\text{one helix alone}}) + RT \ln 2$$

If we conservatively estimate the volume surrounding two nearby cylinders to be 1.5 times that of the volume around each cylinder alone, the resulting energetic gain, at 298 K, is at least $0.4RT$ per mole of counterion. The actual combined volume is likely to be greater than twice the volume about a single cylinder, resulting in even more significant entropy increases. Because there are 36 mol of monovalent counterion/mol of paired helices, this energy becomes quite substantial [≤−9.1 kcal/(mol·pair of helices)]. Similarly, for divalent cations, which are fewer in number, the total energy gained from these entropic effects at 298 K is at least −5.4 kcal/(mol·pair of helices).

Of course, opposing this attractive entropy will be the repulsion between the remaining uncompensated charges on the two nucleic acid duplexes. An upper limit for this repulsion can be obtained by approximating the two duplexes as point charges and then applying Coulomb's law: $\Delta G_{\text{Coulombic}} \leq 322(q_1q_2/Dr_{12})$. In the presence of monovalent salts, the net uncompensated charge on each duplex is [0.76(cations/phosphate) − 1] × 24 phosphates = −5.76. Using a separation between helix axes of 20 Å and a relative dielectric of 78.5, the net Coulombic repulsion is $\Delta G_{\text{Coulombic}} \leq 7.0$ kcal/(mol·pair of helices). Similarly, in divalent salt, $\Delta G_{\text{Coulombic}} \leq 3.9$ kcal/(mol·pair of helices).

The net interaction energy between two duplexes is given by $\Delta G_{\text{interaction}} = \Delta G_{\text{entropic}} + \Delta G_{\text{Coulombic}}$. Using the minimum entropic gain [$\Delta G_{\text{entropic}} \leq -9.1$ kcal/(mol·pair of helices)] and the maximum Coulombic repulsion [$\Delta G_{\text{Coulombic}} \leq 7.0$ kcal/(mol·pair of helices)], we obtain a minimum net

interaction free energy for two duplexes in monovalent salt of $\Delta G_{interaction} \leq -2.1$ kcal/(mol·pair of helices). Similarly, in the presence of divalent cations, the minimum net interaction free energy is given by $\Delta G_{interaction} \leq -1.5$ kcal/(mol·pair of helices). Both of these net energies are substantially greater than physiological *kT* and are conspicuously absent from most models of RNA folding.

Indeed, these numbers represent extremely conservative estimates, and actual values are likely to be substantially more favorable. First, the relative increase in delocalization volume was estimated as 1.5 but is likely to be greater than 2.0 (*21*, *22*), resulting in approximately 6 kcal/(mol·pair of helices) more favorable interaction energy. Also, the Coulombic repulsion term is a significant overestimate as it approximates each helix as a point charge whereas the distribution of charge along the axis of real helices mitigates the repulsion. Furthermore, ionic screening, which also serves to reduce the repulsion between helices, was completely ignored. Favorable Coulombic interactions between the ionic cloud around one helix and the remaining charge on the other helix were also omitted. Correlated dipole effects, which are always favorable and could also favor parallel packing, were not included either. Finally, even slight separations (2−5 Å), as observed in crystal structures, can substantially relieve the Coulombic repulsion between the two helices. A separation of this sort also has the effect of increasing the delocalization volume of the condensed counterions and thus increasing the entropic gain. Despite ignoring all these favorable terms, the net interaction energy between the two duplexes and their counterion clouds is still at least −2.1 kcal/(mol·pair of helices) in monovalent salt and at least −1.5 kcal/(mol·pair of helices) in divalent salt, both should be sufficient to counterbalance the translational entropy lost by the two duplexes upon association (*34*).

SUPPORTING INFORMATION AVAILABLE

Tables containing Nucleic Acid Database (NDB) identifiers for the structures analyzed in this study and crossing angle and separation data extracted from these structures. This material is available free of charge via the Internet at http://pubs.acs.org.

REFERENCES

1. Zuker, M. (*2000*) *Curr. Opin. Struct. Biol. 10*, 303−310.
2. Mathews, D. H., Sabina, J., Zuker, M., and Turner, D. H. (1999) *J. Mol. Biol. 288*, 911−940.
3. Wuchty, S., Fontana, W., Hofacker, I. L., and Schuster, P. (1999) *Biopolymers 49*, 145−165.
4. Gautheret, D., and Gutell, R. R. (1997) *Nucleic Acids Res. 25*, 1559−1564.
5. Crick, F. H. C. (1953) *Acta Crystallogr. 6*, 689−697.
6. Richmond, T. J., and Richards, F. M. (1978) *J. Mol. Biol. 119*, 537−555.
7. Cohen, F. E., Richmond, T. J., and Richards, F. M. (1979) *J. Mol. Biol. 132*, 275−288.
8. Chothia, C., Levitt, M., and Richardson, D. (1977) *Proc. Natl. Acad. Sci. U.S.A. 74*, 4130−4134.
9. Timsit, Y., Westhof, E., Fuchs, R. P., and Moras, D. (1989) *Nature 341*, 459−462.
10. Timsit, Y., Shatzky-Schwartz, M., and Shakked, Z. (1999) *J. Biomol. Struct. Dyn. 16*, 775−785.
11. Cate, J. H., Gooding, A. R., Podell, E., Zhou, K., Golden, B. L., Kundrot, C. E., Cech, T. R., and Doudna, J. A. (1996) *Science 273*, 1678−1685.
12. Ferre-D'Amare, A. R., Zhou, K., and Doudna, J. A. (1998) *Nature 395*, 567−574.
13. Wimberly, B. T., Guymon, R., McCutcheon, J. P., White, S. W., and Ramakrishnan, V. (1999) *Cell 97*, 491−502.
14. Conn, G. L., Draper, D. E., Lattman, E. E., and Gittis, A. G. (1999) *Science 284*, 1171−1174.
15. Manning, G. S. (1977) *Biophys. Chem. 7*, 95−102.
16. Manning, G. S. (1979) *Acc. Chem. Res. 12*, 443−449.
17. Berman, H. M., Olson, W. K., Beveridge, D. L., Westbrook, J., Gelbin, A., Demeny, T., Hsieh, S. H., Srinivasan, A. R., and Schneider, B. (1992) *Biophys. J. 63*, 751−759.
18. Christopher, J. A., Swanson, R., and Baldwin, T. O. (1996) *Comput. Chem. 20*, 339−345.
19. Walther, D., Springer, C., and Cohen, F. E. (1998) *Proteins 33*, 457−459.
20. Cate, J. H., Hanna, R. L., and Doudna, J. A. (1997) *Nat. Struct. Biol. 4*, 553−558.
21. Ray, J., and Manning, G. S. (1997) *Macromolecules 30*, 5739−5744.
22. Ray, J., and Manning, G. S. (1994) *Langmuir 10*, 2450−2461.
23. Bloomfield, V. A. (1997) *Biopolymers 44*, 269−282.
24. Parsegian, V. A., and Rau, D. C. (1984) *J. Cell Biol. 99*, 196s−200s.
25. Manning, G. S. (1996) *Ber. Bunsen. Phys. Chem. 100*, 909−922.
26. Fenley, M. O., Manning, G. S., and Olson, W. K. (1990) *Biopolymers 30*, 1191−1203.
27. Anderson, C. F., and Record, M. T., Jr. (1995) *Annu. Rev. Phys. Chem. 46*, 657−700.
28. Gill, S. J., Richey, B., Bishop, G., and Wyman, J. (1985) *Biophys. Chem. 21*, 1−14.
29. Buchmueller, K. L., Webb, A. E., Richardson, D. A., and Weeks, K. M. (2000) *Nat. Struct. Biol. 7*, 362−366.
30. Russell, R., Millett, I. S., Doniach, S., and Herschlag, D. (2000) *Nat. Struct. Biol. 7*, 367−370.
31. Li, Y., Bevilacqua, P. C., Mathews, D., and Turner, D. H. (1995) *Biochemistry 34*, 14394−14399.
32. Narlikar, G. J., and Herschlag, D. (1996) *Nat. Struct. Biol. 3*, 701−710.
33. Shiman, R., and Draper, D. E. (2000) *J. Mol. Biol. 302*, 79−91.
34. Murphy, K. P., Xie, D., Thompson, K. S., Amzel, L. M., and Freire, E. (1994) *Proteins 18*, 63−67.
35. Gao, Y. G., Robinson, H., Sanishvili, R., Joachimiak, A., and Wang, A. H. (1999) *Biochemistry 38*, 16452−16460.
36. Pan, B., Mitra, S. N., and Sundaralingam, M. (1998) *J. Mol. Biol. 283*, 977−984.

BI001820R